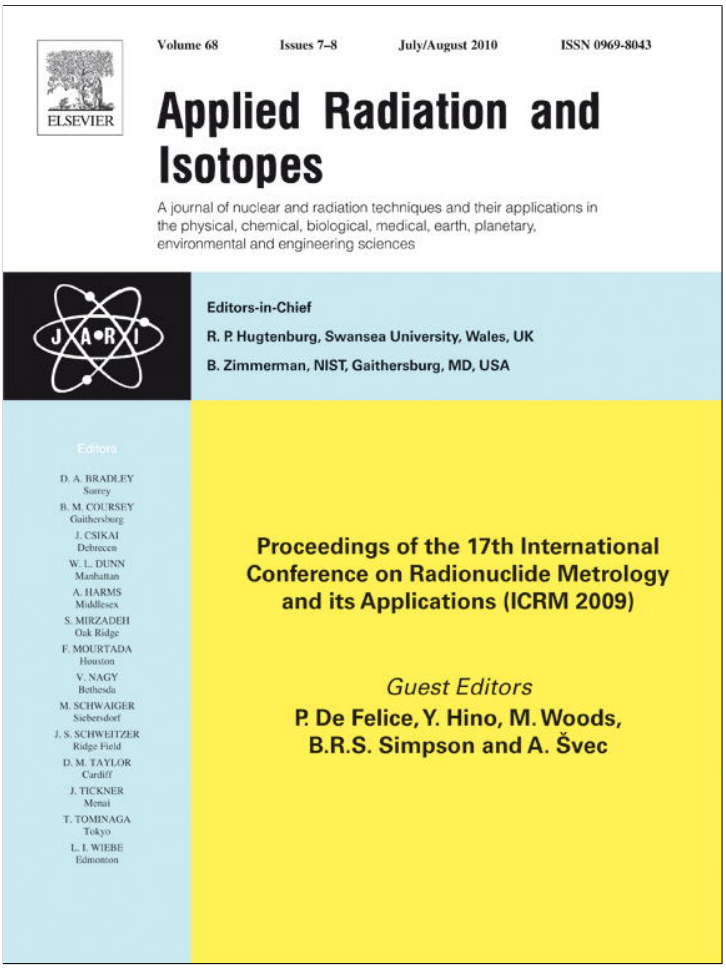

Applied Radiation and Isotopes 68 (2010) 1286–1291

Contents lists available at ScienceDirect

Applied Radiation and Isotopes

journal homepage: www.elsevier.com/locate/apradiso

Absolute $^{108}Ag^{m}$ characterization based on gamma–gamma coincident detection by two NaI(Tl) detectors

Peter Volkovitsky *

National Institute of Standards and Technology, Gaithersburg, MD, USA

A B S T R A C T

A two-dimensional analysis of three coincident γ-rays in $^{108}Ag^{m}$ decay, detected by two NaI(Tl) scintillation detectors, allows a direct measurement of the source activity. A modification of the Eldridge–Crowther formulas derived originally for ^{125}I was done recently for the case of two coincident γ-rays in ^{60}Co decay (Volkovitsky and Naudus, 2009). A similar approach is applied to a more complicated case of three coincident γ-rays in the $^{108}Ag^{m}$ decay. The large number of experimental quantities, measured both in coincidence and anticoincidence modes, allows the determination of both detector efficiencies for all three γ-ray photopeaks and to find the source activity. Results are compared with measurements of the activity of the same source with HPGe detectors.

Published by Elsevier Ltd.

1. Introduction

Photon–photon coincidence counting is one of a few ways for direct measurement of activity in radioactive decays (see, for example, NCRP, 1985; Knoll, 2000). This method is widely used for characterization of ^{125}I by detection of X-ray–γ-ray coincident events (Eldridge and Crowther, 1964; Taylor, 1967; Horrocks and Klein, 1975; Schrader and Walz, 1987; Martin and Taylor, 1992; Lee et al., 2004; Pommé et al., 2005). In case of the coincident emission of several γ-rays, a careful account of Compton scattering should be done. Recently Volkovitsky and Naudus (2009) suggested the modification of the standard Eldridge–Crowther formulas for the case of coincident emission of two γ-rays in ^{60}Co decay. In the present paper a similar approach is applied to the decay of $^{108}Ag^{m}$ with emission of three coincident γ-rays. The two- and one-dimensional analyses of coincidence events together with one-dimensional analysis of anticoincidence events allow to careful separation of photopeaks for each γ-ray and the determination of detection efficiencies and source activity.

2. Formulas for $^{108}Ag^{m}$ decay

In $^{108}Ag^{m}$ electron capture (EC) decay, three γ-rays are emitted in coincident cascade: 433.9, 614.3 and 722.9 keV with 91.3% branching ratio. Let us assume that these cascade γ-rays are non-correlated (γ-ray correlation effects will be discussed later).

Three cascade γ-rays produce twelve two-dimensional photopeaks on a coincident plane. Here upper index 1 denotes the 433.9 keV γ-ray, upper index 2 denotes the 614.3 keV γ-ray, and upper index 3 denotes the 722.9 keV γ-ray. Lower index 1 denotes the first detector and lower index 2 denotes the second detector. If the total rate of decays with emission of cascade γ-rays, in this paper referred to as the 3γ decay rate, is N_0, the count rates in these coincident photopeaks are given by the following formulas:

$$N_c^{i,j} = N_0 \varepsilon_1^{ip} \varepsilon_2^{jp} (1-\varepsilon_1^{kt}-\varepsilon_2^{kt}) \quad (1)$$

Values $N_c^{i,j}$ are the count rates of coincident events when γ-ray in the photopeak i is detected by the first detector and γ-ray in the photopeak j is detected by the second detector; $k \neq i, j$. ε_l^{ip} (i=1,2,3; l=1,2) are the detection probabilities for three γ-rays in photopeaks by detector l, and ε_l^{it} (i=1,2,3; l=1,2) is the total detection probability of γ-ray i by detector l. Note that $(1-\varepsilon_1^{kt}-\varepsilon_2^{kt})$ is the probability that γ-ray k is not detected by either detector.

$$N_c^{(ij),k} = N_0 \varepsilon_1^{ip} \varepsilon_1^{jp} \varepsilon_2^{kp} \quad (2)$$

Values $N_c^{(ij),k}$ are the coincident summation count rates. Two γ-rays, i and j, are detected by the first detector in the photopeak areas, and γ-ray k is detected by the second detector in the photopeak area.

Twelve two-dimensional coincident photopeaks are described by six photopeak detection probabilities ε_l^{ip} (i=1,2,3; l=1,2) and by six total detection probabilities ε_l^{it}. Not all of Eqs. (1) and (2) are independent, and thus Eqs. (1) and (2) do not allow determining the 3γ decay rate N_0.

The photopeaks and summation peaks in detector l (l=1, 2) can be expressed in terms of the same detection efficiencies as

* Tel.: +1 301 975 5527; fax: +1 301 926 7416.
E-mail address: peter.volkovitsky@nist.gov

0969-8043/$ - see front matter Published by Elsevier Ltd.
doi:10.1016/j.apradiso.2009.12.004

follows:

$$N_l^i = N_0\varepsilon_l^{ip}(1-\varepsilon_l^{jt})(1-\varepsilon_l^{kt}), \quad N_l^{i,j} = N_0\varepsilon_l^{ip}\varepsilon_l^{jp}(1-\varepsilon_j^{kt}), \quad N_l^{1,2,3} = N_0\varepsilon_l^{1p}\varepsilon_l^{2p}\varepsilon_l^{3p} \tag{3}$$

The difference between the total count rate in detector j and the coincidence count rate in the same detector is the anticoincidence count rate. The anticoincidence event count rates in photopeaks and in summation peaks in detector j can be written as:

$$N_{lac}^i = N_0\varepsilon_l^{ip}(1-\varepsilon_1^{jt}-\varepsilon_2^{jt})(1-\varepsilon_1^{kt}-\varepsilon_2^{kt}), \quad N_{lac}^{i,j} = N_0\varepsilon_l^{ip}\varepsilon_l^{jp}(1-\varepsilon_1^{kt}-\varepsilon_2^{kt}),$$

$$N_{lac}^{1,2,3} = N_0\varepsilon_l^{1p}\varepsilon_l^{2p}\varepsilon_l^{3p} \tag{4}$$

Again not all Eqs. (3) are independent. However, now the number of Eqs. (1)–(3) is equal to 26 and is bigger than the number of unknowns (ε_l^{it}, ε_l^{ip}, and N_0), which is equal to 13. Thus the 3γ decay rate, $N_{0,}$ can be calculated. Since the number of equations is larger than the number of unknowns, the unknowns should be determined by minimization of

$$\chi^2 = \sum_{m=1}^{m=26}(N_{m,\exp}-N_{m,th})^2 \tag{5}$$

Here $N_{\exp}$ is the measured count rate in phoptopeaks (total, coincidence or anticoincidence) and N_{th} is given by Eqs. (1)–(3). The summation goes over all 26 equations.

For successful minimization, the first approximations for ε_j^{it}, ε_j^{ip}, and N_0 have to be defined. From Eqs. (2) and (4) it is easy to find the total detection probabilities ε_j^{it}. Consider the four equations:

$$N_1^{1,2} = N_0\varepsilon_1^{1p}\varepsilon_1^{2p}(1-\varepsilon_1^{3t}), \quad N_2^{1,2} = N_0\varepsilon_2^{1p}\varepsilon_2^{2p}(1-\varepsilon_2^{3t}),$$

$$N_{1ac}^{1,2} = N_0\varepsilon_1^{1p}\varepsilon_1^{2p}(1-\varepsilon_1^{3t}-\varepsilon_2^{3t}), \quad N_{2ac}^{1,2} = N_0\varepsilon_2^{1p}\varepsilon_2^{2p}(1-\varepsilon_1^{3t}-\varepsilon_2^{3t}) \tag{6}$$

Denoting $R_1^{1,2} = N_1^{1,2}/N_{1ac}^{1,2}$ and $R_2^{1,2} = N_2^{1,2}/N_{2ac}^{1,2}$, we obtain two equations for two unknowns, ε_1^{3t} and ε_2^{3t}:

$$\frac{1-\varepsilon_1^{3t}}{1-\varepsilon_1^{3t}-\varepsilon_2^{3t}} = R_1^{1,2} \quad \text{and} \quad \frac{1-\varepsilon_2^{3t}}{1-\varepsilon_1^{3t}-\varepsilon_2^{3t}} = R_2^{1,2} \tag{7}$$

The solution of Eq. (7) has the form:

$$\varepsilon_1^{3t} = \frac{R_2^{1,2}-1}{R_1^{1,2}+R_2^{1,2}-1} \quad \text{and} \quad \varepsilon_2^{3t} = \frac{R_1^{1,2}-1}{R_1^{1,2}+R_2^{1,2}-1} \tag{8}$$

The detection probabilitiesε_1^{1t}, ε_2^{1t}, ε_1^{2t} and ε_2^{2t} can be found in a similar way.

In this derivation $R_1^{1,2}$ and $R_2^{1,2}$ were calculated using the count rates in the summation peaks, which are less than the count rates in the photopeaks. The same ratios can be calculated using the

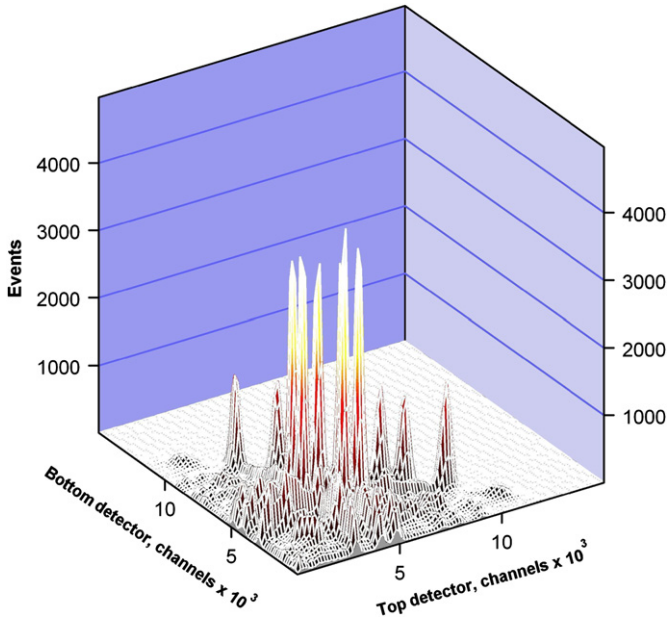

Fig. 2. The two-dimensional histogram of coincident events obtained for the middle position of a source. The 2D matrix was re-binned for 300×300 bins. The numbers along the axes are bins of the original $20\,000 \times 20\,000$ matrix (in units 10^3).

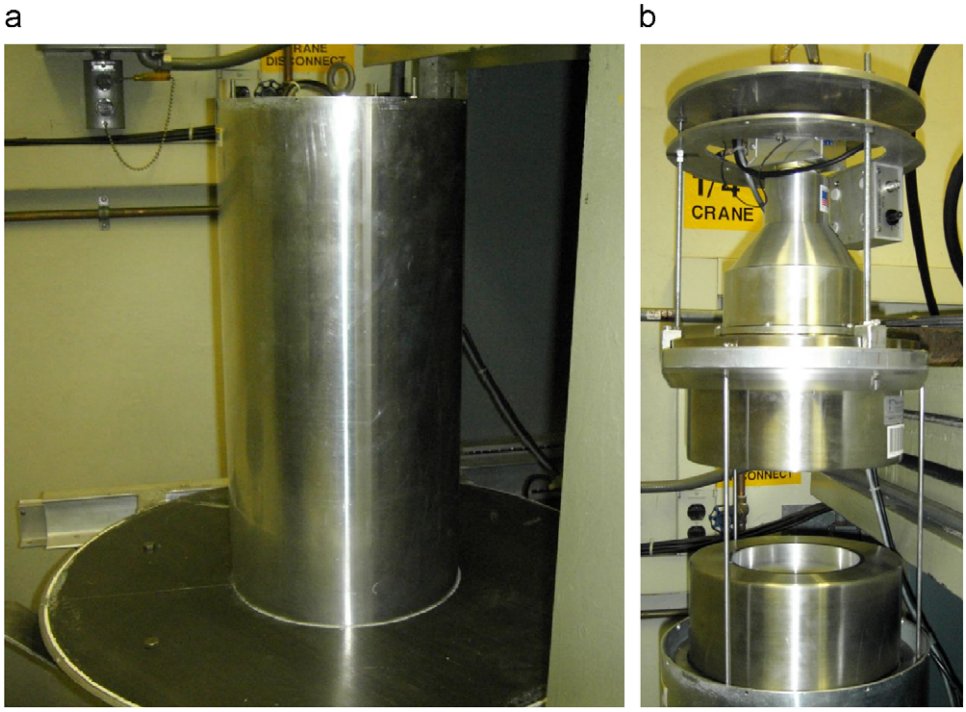

Fig. 1. NIST NaI(Tl) coincident detector: (a) closed and (b) opened.

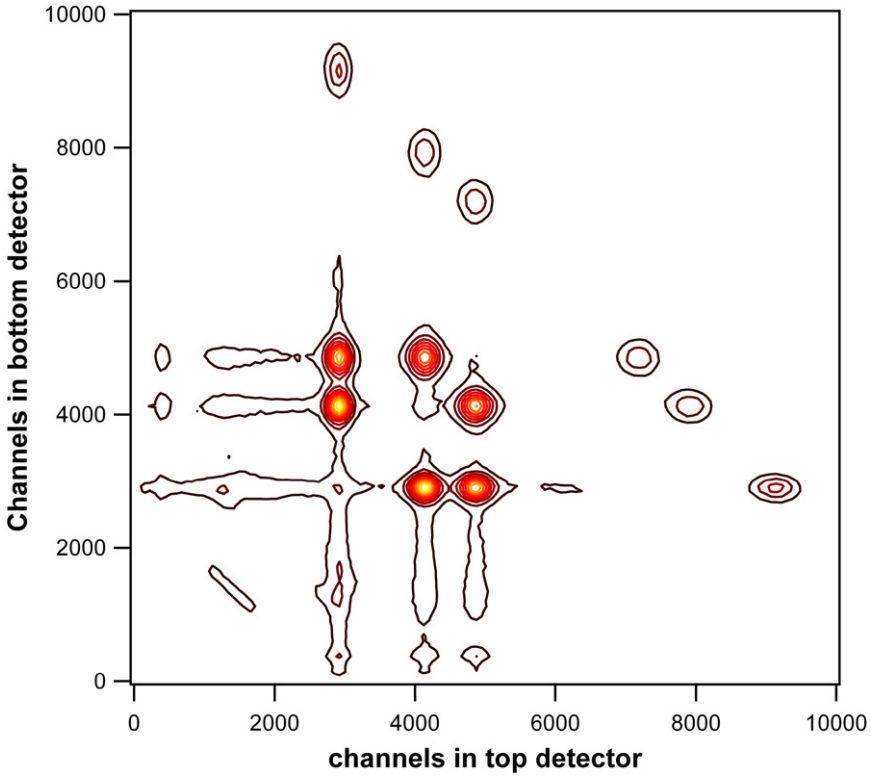

Fig. 3. Contour plot for a two-dimensional histogram of coincident events shown in Fig. 2. Six coincident peaks and six coincident summation peaks are clearly seen.

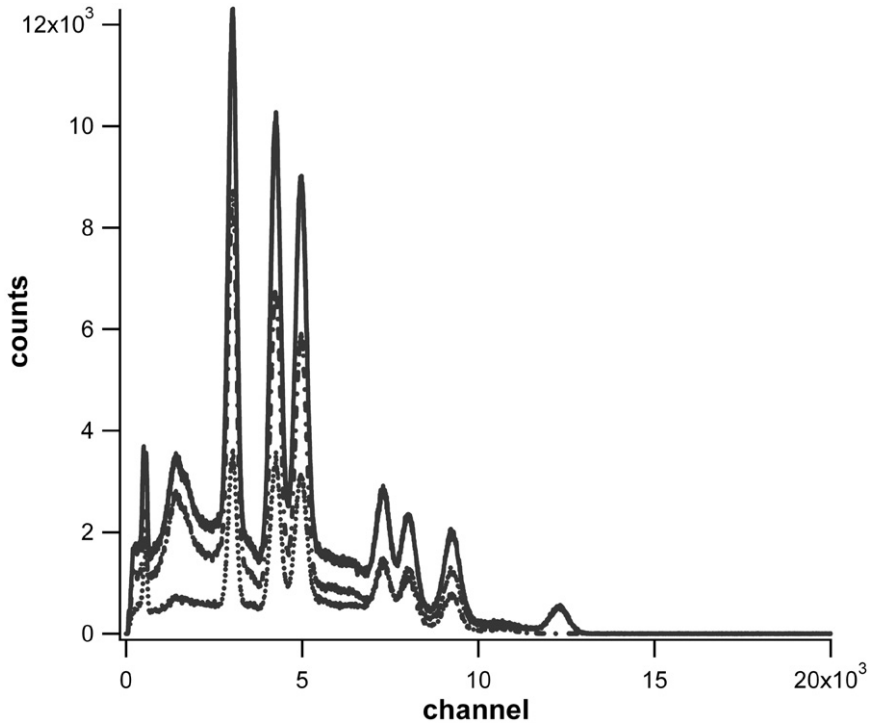

Fig. 4. Spectra detected in the top detector with source in the middle position with background subtracted. The solid line is the total number of counts in detector. The dotted line represents the spectrum of anticoincidence counts, when energy detected in the second detector is zero. The dash-dotted line is the difference between the two spectra. This spectrum can also be obtained by projection of the two-dimensional histogram of coincident events, shown in Fig. 2, onto the top detector axes. Three γ-ray peaks and three summation peaks are clearly seen. Note that the triple summation peak is absent in coincident events.

Table 1
The numbers of counts in two-dimensional coincidence peaks.

Peaks	Source position		
	Bottom	Middle	Top
1,2	165 082	138 029	132 070
2,1	131 938	140 705	134 091
1,3	137 602	133 019	132 007
3,1	129 532	133 467	137 845
2,3	143 174	143 898	142 530
3,2	139 842	145 420	142 120
(12),3	55 865	64 005	68 742
3,(21)	72 602	63 442	57 702
(13),2	53 602	62 446	67 539
2,(13)	74 299	61 254	56 860
(23),1	50 692	60 875	67 440
1,(23)	71 449	59 114	52 448

Table 2
The numbers of counts in one-dimensional peaks.

Det/Peak		Bottom				Middle				Top			
		Total	Coin	Antic	Dif	Total	Coin	Antic	Dif	Total	Coin	Antic	Dif
1	1	641 573	494 209	148 432	−1068	647 707	465 447	176 144	6116	635 275	454 951	175943	4381
	2	637 000	477 850	171 190	−12 040	657 844	459 024	201 317	−2497	653 030	443 689	213600	−4259
	3	607 421	448 337	175 324	−16 240	638 901	416 572	209 777	12 552	639 796	421 162	226900	−8266
	12	237 061	136 248	105 732	−4919	304 589	158 264	148 112	−1787	343 924	171 410	172290	224
	13	204 678	106 492	96 791	1395	263 086	126 509	135 709	868	307 128	145 028	161867	233
	23	178 203	79 672	98 621	−90	237 723	96 512	141 605	−394	279 116	109 223	170197	−304
	123	60 403		59 666	737	68 293	0	67 612	681	88 736		87941	795
2	1	617 695	447 775	183 613	−13 693	628 191	470 874	168 549	−11 232	624 126	476 954	153 556	−6384
	2	652 388	426 402	225 065	921	651 258	456 932	192 705	1621	627 703	461 876	177 590	−11 763
	3	645 676	404 900	241 638	−862	634 531	429 177	202 900	2454	618 559	430 836	184 370	3353
	12	366 157	185 846	178 940	1371	301 089	162 767	146 990	−8668	255 699	143 680	114 809	−2790
	13	329 333	152 835	177 028	−530	253 759	120 992	124 967	7800	219 536	110 013	107 935	1588
	23	301 205	116 875	184 432	−102	231 659	94 979	136 965	−285	199 971	84 153	108 973	6845
	123	142 807		141 432	1375	63 219	0	62 341	878	47 743		46 997	746

The difference between the total and the sum of coincidence and anticoincidence counts in each peak should be zero. The non-zero values demonstrate fit accuracies. The average relative difference across Table 2 data is 1%.

count rates in the photopeaks. Let us first consider the ratios:

$$R_1^1 = \frac{N_1^1}{N_{1ac}^1} = \frac{(1-\varepsilon_1^{2t})(1-\varepsilon_1^{3t})}{(1-\varepsilon_1^{2t}-\varepsilon_2^{2t})(1-\varepsilon_1^{3t}-\varepsilon_2^{3t})} \tag{9a}$$

$$R_1^2 = \frac{N_1^2}{N_{1ac}^2} = \frac{(1-\varepsilon_1^{1t})(1-\varepsilon_1^{3t})}{(1-\varepsilon_1^{1t}-\varepsilon_2^{1t})(1-\varepsilon_1^{3t}-\varepsilon_2^{3t})} \tag{9b}$$

$$R_1^3 = \frac{N_1^3}{N_{1ac}^3} = \frac{(1-\varepsilon_1^{1t})(1-\varepsilon_1^{2t})}{(1-\varepsilon_1^{1t}-\varepsilon_2^{1t})(1-\varepsilon_1^{2t}-\varepsilon_2^{2t})} \tag{9c}$$

It is obvious that

$$(R_1^{1,2})^2 = \left(\frac{1-\varepsilon_1^{3t}}{1-\varepsilon_1^{3t}-\varepsilon_2^{3t}}\right)^2 = \frac{R_1^1 R_1^2}{R_1^3} \tag{10}$$

Similar relations can be written for all other ratios. Thus, $R_1^{1,2}$ and other ratios and total detection efficiencies can be calculated using only the high-statistics data from photopeaks.

Now from the coincidence data we can find the photopeak detection probabilities, ε_l^{ip}. From Eqs. (1) and (2) it follows that

$$\varepsilon_1^{1p} = \frac{N_c^{(12),3}}{N_c^{2,3}}(1-\varepsilon_1^{1t}-\varepsilon_2^{1t}) \tag{11}$$

All other detection probabilities ε_l^{ip} can be found in a similar way. After all detection probabilities are found, the decay rate N_0 can easily be determined. Values for the detection probabilities and decay rate N_0 found from Eqs. (8) and (11) are used as the first approximation for minimization of χ^2in Eq. (5).

All γ-rays are emitted in E2-type transitions with ΔJ=2, ΔP=0. Because of this, the correlation function $W(\cos\theta)$between γ-rays is an even function of $\cos\theta$, where θ is the angle between the two γ-rays (see Gill, 1975):

$$W(\cos\theta) = 1 + a_2 P_2(\cos\theta) + a_4 P_4(\cos\theta) \tag{12}$$

where $P_n(\cos\theta)$ is a Legendre polynomial of n-th order. Since function $W(\cos\theta)$ is an even function of $\cos\theta$, if the source is located in the center of symmetry between the two identical detectors, the probabilities of the second gamma detection in the same or opposite detector are equal, and Eqs. (1)–(4) are still valid.

3. Experimental data and results

Experimental data were obtained with the NIST 8″ NaI(Tl) coincident detector, shown in Fig. 1.

Two NaI(Tl) crystals 8″ in diameter and 6″ thick are coupled with 5″ PMTs. The sample cavity between detectors has a 5″ diameter and 1.5″ height. Detectors are placed inside a low-background chamber, but for loading and unloading the source, they can be moved out of the chamber and opened using a pneumatic crane. Detectors are connected to spectroscopic amplifiers and to a PIXIE-4 data acquisition module www.xia.

Table 3
Results of calculations of $^{108}Ag^{m}$ source 3γ decay rate and NaI(Tl) detector efficiencies for the source placed in three positions.

	Bottom		Middle		Top	
	Initial	Final	Initial	Final	Initial	Final
ε_1^{1t}	0.259	**0.240**	0.292	**0.299**	0.337	**0.323**
ε_1^{2t}	0.289	**0.278**	0.347	**0.316**	0.353	**0.343**
ε_1^{3t}	0.318	**0.266**	0.338	**0.320**	0.381	**0.365**
ε_2^{1t}	0.331	**0.361**	0.286	**0.283**	0.259	**0.241**
ε_2^{2t}	0.375	**0.348**	0.316	**0.316**	0.306	**0.294**
ε_2^{3t}	0.378	**0.386**	0.340	**0.327**	0.309	**0.298**
ε_1^{1p}	0.160	**0.234**	0.188	**0.274**	0.195	**0.307**
ε_1^{2p}	0.136	**0.219**	0.162	**0.268**	0.178	**0.300**
ε_1^{3p}	0.099	**0.210**	0.146	**0.254**	0.159	**0.279**
ε_2^{1p}	0.213	**0.305**	0.180	**0.270**	0.161	**0.252**
ε_2^{2p}	0.175	**0.319**	0.150	**0.263**	0.135	**0.234**
ε_2^{3p}	0.132	**0.292**	0.138	**0.246**	0.123	**0.225**
N_0, s^{-1}	800	**860**	800	**843**	800	**834**
A, Bq		**942**		**923**		**913**

Activity is the count rate divided by the 91.3% branching ratio.

Table 4
Uncertainty budget for $^{108}Ag^{m}$ source activity measurement by the $\gamma-\gamma$ coincidence method.

Input quantity x_i, the source of uncertainty (and individual uncertainty components where appropriate)	Method used to evaluate $u(x_i)$, the standard uncertainty of x_i (a) denotes evaluation by statistical methods (b) denotes evaluation by other methods	Relative uncertainty of input quantity, $u(x_i)/x_i$, (%)	Relative sensitivity factor, $\lvert\partial y/\partial x_i\rvert$ (x_i/y)	Relative uncertainty of output quantity, $u_i(y)/y$, (%)
Number of counts in 1D peaks	Statistical (a)	0.2	1.0	0.2
Number of counts in 2D peaks	Statistical (a)	0.9	1.0	0.9
Uncertainty in fit consistency	Estimated (b)	1.0	1.0	1.0
Uncertainty in subtraction constants	Estimated (b)	10	0.06	0.6
Uncertainty in branching ratio	Estimated (b)	1.0	1.0	1.0
Accuracy of parameter fit	Estimated (b)	1.5	1.0	1.5
Combined Relative Standard Uncertainty of the Evaluation (k=1)				**2.3**

com/index.html. Pulses from both detectors are recorded and analyzed using IGOR software (www.wavemetrics.com)[1].

One $^{108}Ag^{m}$ source was measured in three positions inside the detector: close to the center of the sample chamber, and placed at the top and at the bottom of the sample chamber. In each measurement the same total number of events, approximately 10^7 events, was acquired. The measurement time depended on source position and was 6089 s for the bottom position, 6114 s for the middle position and 6093 s for top position. For each source position, three spectra were measured: spectra for the top and bottom detectors and a two-dimensional coincidence spectrum. The background was measured in the same way as samples were measured and was subtracted bin-by-bin from all spectra. The number of bins in the spectra, recorded by PIXIE-4 in the energy interval 0–3000 keV, was 20,000. Spectra were re-binned before data processing. For one-dimensional spectra, the number of bins was reduced to 4000. The two-dimensional spectrum matrix had 2000×2000 bins. In Fig. 2, a typical example of two-dimensional $^{108}Ag^{m}$ spectrum is shown (Fig. 3).

The structure of coincident events can be seen also on a contour plot:

Examples of one-dimensional spectra are shown in Fig. 4.

All two-dimensional peaks were fitted by two-dimensional Gaussian formula. With a 2000×2000 matrix for coincidence events, the average number of degrees of freedom for a two-dimensional fit was about 1000.

The triple summation peak in total and anticoincidence events was fitted by the one-dimensional Gaussian curve. Three double summation peaks in total, coincidence, and anticoincidence one-dimensional spectra were fitted by the sum of three Gaussians and a constant.

Two close peaks at 614.3 and 722.9 keV were fitted by the sum of two Gaussians and a constant. The 433.9 keV peak was fitted by a sum of a Gaussian and a constant.

Numbers of events in each peak were calculated based on fitted parameters for this peak. The results for two-dimensional peaks are shown in Table 1. Notations for peaks are the same as in Eqs. (1), (2).

The numbers of counts in one-dimensional peaks are shown in Table 2.

The results of optimization (minimization of χ^2 in Eq. (5)) together with the first approximation calculated according Eqs. (8) and (11) are shown in Table 3.

For fits performed for all three source positions the value of χ^2 per degree of freedom was about 30. The difference in activity of the source measured in the top, middle, and bottom position may be due to $\gamma-\gamma$ correlations.

The source activity was independently measured by HPGe detectors. The average result of six HPGe measurements (three γ-rays and two detectors) was 923 ± 97 Bq (k=1).

[1] Certain commercial equipment, instruments, software, or materials are identified in this paper to specify adequately the experimental procedure. Such identification does not imply recommendation or endorsement by the National Institute of Standards and Technology, nor does it imply that the materials or equipment identified are necessarily the best available for the purpose

The uncertainty budget of measurements with NaI(Tl) detectors is given in Table 4.

Acknowledgements

The author is grateful to David Brown for the $^{108}Ag^{m}$ source, to Leticia Pibida for measurements performed by HPGe and discussions, and to Philip Naudus for help with sample measurements. I am also grateful to Heather Chen-Mayer, Ryan Fitzgerald, Robin Hutchinson, Jerry LaRosa, and Mike Unterweger for support and discussions.

References

Eldridge, J.S., Crowther, P., 1964. Absolute determination of ^{125}I in clinical applications. Nucleonics 22, 56–59.
Gill, R.D., 1975. Gamma-ray Angular Correlations. Academic Press Inc., London.
Horrocks, D.L., Klein, P.R., 1975. Theoretical considerations for standardization of ^{125}I by the coincidence method. Nucl. Instr. and Meth. 124, 585–589.
Knoll, G.F., 2000. Radiation Detection and Measurement, 3rd ed. John Wiley & sons, Inc.
Lee, J.M., Lee, K.B., Lee, M.K., et al., 2004. Standardization of ^{125}I and ^{238}Pu. Appl. Radiat. Isot. 60, 397–401.
Martin, R.H., Taylor, J.C.V., 1992. The standardization of ^{125}I: a comparison of three methods. Nucl. Instr. and Meth. A 312, 64–66.
NCRP Report 58, 1985. A handbook of radioactivity measurements.
Pommé, S., Altzitzoglou, T., Van Ammel, R., Sibbens, G., 2005. Standardization of ^{125}I using seven techniques for radioactivity measurement. Nucl. Instr. and Meth. A 544, 584–592.
Schrader, H., Walz, K.F., 1987. Standardization of ^{125}I by photon-photon coincidence counting and efficiency extrapolation. Appl. Radiat. Isot. 38, 763–766.
Taylor, J.G.V., 1967. X-ray–X-ray coincidence counting methods for the standardization of ^{125}I and ^{197}Hg, in Standardization of Radionuclides, IAEA, Vienna pp. 341–355.
Volkovitsky, P., Naudus, P., 2009. Absolute ^{60}Co characterization based on gamma–gamma coincident detection by two NaI(Tl) detectors. Nucl. Instr. and Meth. A 607, 568–572.
〈www.xia.com/index.html〉.
〈www.wavemetrics.com〉.

Discussion

Q (Heinrich Schrader (PTB)): My major problem with such a method is in the determination of the background below single photon energy peaks. Several authors used such a method in the 1950s and 1960s, but due to this problem, the method was abandoned in favor of the 4pb-g coincidence technique. I don't see how you can avoid of this problem. One condition, for example, would be that you have symmetrical counting efficiency for the two detectors, for each peak.

A (Peter Volkovitsky (NIST)): In the 1950s, there were no digital electronics, and there was no way to view the two-dimensional coincidence plots. For coincident events, in the two-dimensional plot, the background is negligible and the problem vanishes. Of course you are right, for a one-dimensional spectrum the background presents a problem, and I tried to estimate the uncertainty that arose from my definition of the background that rather high and of the level of several percent. But in the two-dimensional space; there is no background; that is the difference between this work, and what was done before.

Q (Phillipe Cassette (LNHB)): Your coincidence equation is only correct if you assume that there is no correlation between the two detectors. So what happens in the case where there is a Compton interaction in one detector, and the scattered photon is subsequently detected by the other detector. Is the resolution of the sodium iodide detector sufficient to reject this type of event?

A (Peter Volkovitsky (NIST)): Scattered events are readily resolved from the photo-peaks, and are concentrated around 200 keV, whereas the photo-peaks reside in the range of 400 to 700 keV.

I have presented the equation for correlation between detectors, and in this case the correlation cancels if the source is located centrally between the two identical detectors. I have two identical detectors and at least the double correlation between the two gammas vanish. I am not so sure about triple correlation, but triple correlations are much less important. However, there are correlations, and of course the equations were written under the assumption that the events are independent. Fortunately, due to the E-2 transition, these correlations vanish with the source in the central location.

Q (Octavian Sima (Bucharest University)): I would like to again ask about the problem of the scattering of one photon from one detector to the other.

In computing the probability of not detecting a photon, one must consider the following independent cases: the photon is not detected by either detector; it is detected in one only, in the other only, or in both detectors. That is, the probability of not detecting a photon is one minus the probability of non-detection in one, plus the probability of non-detection in the second, plus the probability of non-detection in both. If you define the total efficiency by the probability of photon detection in a single detector, this includes the probability of detection in both.

A (Peter Volkovitsky (NIST)): The total probabilities of photon detection are not related directly to my observed counts, they are just the parameters of the model. I agree with you that the model may be modified to take into account what you have just said, but in the first approximation, I have determined these parameters from fits as they are not known *a priori*. From this point of view, the mistake, which I have made in the simplified model, is not so big.